

## Periodic step arrays on the aperiodic *i*-Al-Pd-Mn quasicrystal surface at high temperature

Y. Sato,<sup>1,2</sup> B. Ünal,<sup>3,4</sup> T. A. Lograsso,<sup>4</sup> P. A. Thiel,<sup>3,5,4</sup> A. K. Schmid,<sup>2</sup> T. Duden,<sup>2</sup> N. C. Bartelt,<sup>6</sup> and K. F. McCarty<sup>6</sup>

<sup>1</sup>Department of Physics, University of California, Davis, California 95616, USA

<sup>2</sup>National Center for Electron Microscopy, Lawrence Berkeley National Laboratory, Berkeley, California 94720, USA

<sup>3</sup>Department of Materials Science and Engineering, Iowa State University, Ames, Iowa 50011, USA

<sup>4</sup>Ames Laboratory, Ames, Iowa 50011, USA

<sup>5</sup>Department of Chemistry, Iowa State University, Ames, Iowa 50011, USA

<sup>6</sup>Sandia National Laboratories, Livermore, California 94551, USA

(Received 2 September 2009; revised manuscript received 18 March 2010; published 12 April 2010)

We have observed the configuration and motion of surface steps on the aperiodic icosahedral (*i*-) Al-Pd-Mn quasicrystal using low-energy electron microscopy and scanning tunneling microscopy. As the quasicrystal is cooled from high temperature, bulk vacancies migrate to the surface causing the surface to be etched. Surprisingly, this etching occurs by two types of steps with different heights moving in different directions with different velocities. The steady-state surface morphology is a uniformly spaced rhomboidal step network. This network requires that the layer stacking near the surface deviates from the bulk quasicrystal stacking.

DOI: [10.1103/PhysRevB.81.161406](https://doi.org/10.1103/PhysRevB.81.161406)

PACS number(s): 68.35.bd, 61.72.jd, 66.30.Lw, 68.37.Nq

Many metal surfaces, including quasicrystals (QCs), are commonly prepared by procedures that involve annealing well above room temperature (RT). At such high temperatures (HTs), surface smoothing occurs by mass transport along the surface and through the bulk.<sup>1</sup> In materials where the formation energy of thermal defects is small, changing temperature can also cause a substantial flow of mass between the surface and bulk. Here we show that understanding the motion of surface steps due to this bulk-surface exchange is particularly crucial to understand the morphology of *i*-Al-Pd-Mn QC surfaces. Furthermore, we propose that the step structure gives insight into the HT termination of the QC surface.

The *i*-Al-Pd-Mn QC surface has been intensely studied near and below RT.<sup>2–9</sup> Many studies have addressed the central question of whether the bulk, aperiodic structure continues unperturbed to the surface. That is, whether the surface is bulk truncated, as if made by cleaving a fixed, bulk slab. Scanning tunneling microscopy (STM) images at RT showing a Fibonacci sequence of two step heights have been presented as evidence that the surface is bulk truncated.<sup>3</sup> Occasional deviations from the Fibonacci sequence have been interpreted in terms of phason walls—defects in the stacking sequence of the QC layers.<sup>10,11</sup> However, the spatial extent or density of these phason walls is uncertain. Furthermore, while *i*-Al-Pd-Mn surfaces typically are prepared by HT annealing, little is known about the HT QC surface. Here, we present low-energy electron microscopy (LEEM) observations of the fivefold surface of *i*-Al-Pd-Mn QC at HT. We find that a very large amount of mass flows between the bulk and surface when temperature is changed, causing steps to move. These moving steps evolve to form a remarkably periodic network of steps with two heights. The existence of this network implies deviations from the bulk stacking-layer sequence near the surface.

LEEM and STM measurements were conducted in separate systems using different *i*-Al-Pd-Mn samples but similar preparation methods. The single crystals of *i*-Al<sub>70.2</sub>Pd<sub>20.5</sub>Mn<sub>9.3</sub> QC with the surface oriented perpendicular to a fivefold axis were grown at the Ames Laboratory

Materials Preparation Center and polished to a mirror finish using 6, 1, and 0.25  $\mu\text{m}$  diamond paste on Texmet cloth. The LEEM sample temperature was measured with a C-type thermocouple welded to a washer in thermal contact with the crystal and was calibrated using a two-color optical pyrometer. The LEEM data were obtained from surfaces prepared by a combination of (i) cycles of short sputtering (2–20 min) using 1.5 kV Ar ions at RT and annealing (5–10 min) up to 930 K or (ii) long sputtering (30 min to several hours) followed by annealing up to 930 K. Typically, LEEM experiments started as the sample temperature was being raised to the annealing temperature. Similar observations were obtained from a slightly different method, i.e., (iii) sputtering for 20–30 min followed by annealing up to  $\sim$ 900 K for 2 to 2.5 h. The STM sample was prepared similarly to method (iii), as detailed in Ref. 12. All LEEM images presented here were formed from specularly reflected electrons.

We first show that the HT QC surface is distinct from the RT QC surface. Figure 1 shows LEEM images at (a) 905 K and (b) RT. At 905 K, the main feature on the surface is an array of dark lines. As established using Ag decoration,<sup>13</sup> these dark lines mark the location of surface steps. All of the intervening terraces have the same LEEM intensity. This spatial uniformity is difficult to reconcile with bulk-truncated models because each terrace would then have a different alloy composition and atomic structure.<sup>15–17</sup> Since low-energy electrons are very sensitive to small differences in composition and structure,<sup>18</sup> each terrace would appear with a different intensity that would vary with electron energy.<sup>19</sup> Nevertheless, the *i*-Al-Pd-Mn surface at HT shows no spatial variation in the LEEM intensity at any electron energy, indicating a uniform surface termination.

In contrast, Fig. 1(b) shows that the RT QC surface has a different appearance. Gradients of LEEM contrast occur between adjacent terraces separated by a step and even along single terraces. The dissimilar nature of the RT and HT surfaces is also established by large differences in the intensity of low-energy electron diffraction (LEED) as a function of electron energy, i.e., LEED IV curves, as shown in Fig. 1(d). Our RT QC surface consistently reproduced the LEED IV

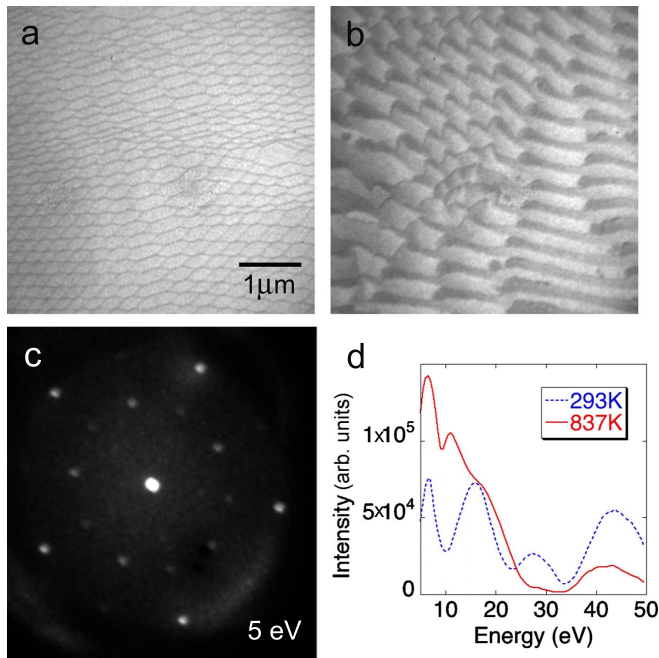


FIG. 1. (Color online) LEEM images of fivefold surface of *i*-Al-Pd-Mn QC. (a) At 905 K, the surface steps form both rhomboidal (area near lower left) and hexagonal meshes (most other areas). Every terrace has the same contrast. (b) At 300 K, the surface termination is no longer uniform. (c) Fivefold LEED pattern at 837 K from a surface with uniform LEEM contrast. (d) Different LEED IV response of the specular beam (00000) (Ref. 5) at 837 K and RT.

curves previously reported.<sup>4,5</sup> The LEED pattern in Fig. 1(c) shows that the fivefold surface symmetry is still present at HT. These two results establish that our sample is a QC and not a periodic material such as the well-studied “approximant” phases of the *i*-Al-Pd-Mn quasicrystal,<sup>20</sup> whose LEED patterns are tenfold symmetric at all electron energies.<sup>21</sup>

The surface steps move markedly when temperature is changed. Figure 2 is a sequence of LEEM images that shows the step motion as temperature oscillated around 906 K. The arrows in Fig. 2(a) indicate the general uphill step direction.<sup>13</sup> The steps advance during heating and retract during cooling relative to the pinning site, which acts as a fiducial. The motion is reversible with temperature, suggesting that it is caused by mass exchange with the bulk and that sublimation is small at this temperature. The mass-flow direction establishes that the thermal defects in the QC are vacancy-like, consistent with previous observations.<sup>22</sup> Vacancies are generated at the surface with increasing temperature to supply the vacancies needed to equilibrate the bulk, causing the steps to advance.<sup>1</sup>

We next establish that the HT QC surface has a remarkable array of surface steps whose configuration is determined by the step motion. After cooling some from the annealing temperature, the steps of the HT phase become increasingly arranged in a rhomboidal mesh [area near lower left of Fig. 1(a)]. As the defects that pin step motion were reduced with more sputter/anneal cycles, the fraction of the surface covered by this mesh increased. Eventually most of the surface was covered by the mesh. In each defect-free region covered

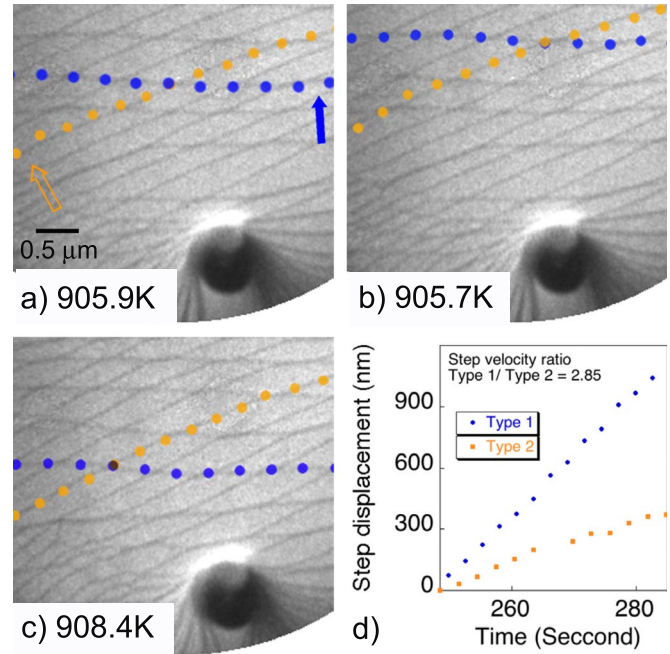


FIG. 2. (Color online) Horizontal steps (type 1) move faster than inclined steps (type 2) following a temperature change. Arrows indicate uphill directions. The dotted lines track the same step. [(a) and (b)] Steps retract during cooling. [(b) and (c)] Steps advance during heating. A video version of a similar data set is available in the supplemental material (Ref. 25). (d) Step position vs time from 907.5 to 906.1 K.

with the mesh, the step spacing is very uniform,<sup>23</sup> i.e., periodic. Thus, the mesh appears to be the steady-state morphology of the HT QC surface on cooling.

When heating adds material to the surface, in contrast, the steps tend to bunch together, as seen in Fig. 2 and the supplemental video.<sup>25</sup> This bunching is most prominent near pinning defects, where the number of bunched steps increased after a temperature rise. Heating also can convert some regions of rhomboidal mesh to hexagons. Two sides of the hexagons form by bunching steps of the rhomboidal network. The bunching is gradually undone on subsequent cooling, restoring the rhomboidal mesh.<sup>24</sup>

Remarkably, the rhomboidal mesh consists of two different types of steps that move with different velocities during heating or cooling. Figure 2(d) shows the time-dependent displacement for the two step types. The velocity ratio in Fig. 2 is 2.9, although the ratio varies with step environment and temperature.<sup>25</sup> The existence of two velocities suggests that the mesh is composed of two step types with different structures.

We propose that this striking step ordering and bunching are caused by an effective Ehrlich-Schwoebel barrier for atomic attachment to steps.<sup>26</sup> Suppose (ignoring for simplicity the complexities inherent in a multicomponent alloy) that the vacancies needed to equilibrate the bulk vacancy concentration are created or destroyed uniformly on each terrace. This creation/destruction supplies a uniform material flux to each terrace, which then diffuses to the step edge to be incorporated. If the barriers for incorporation from the terrace

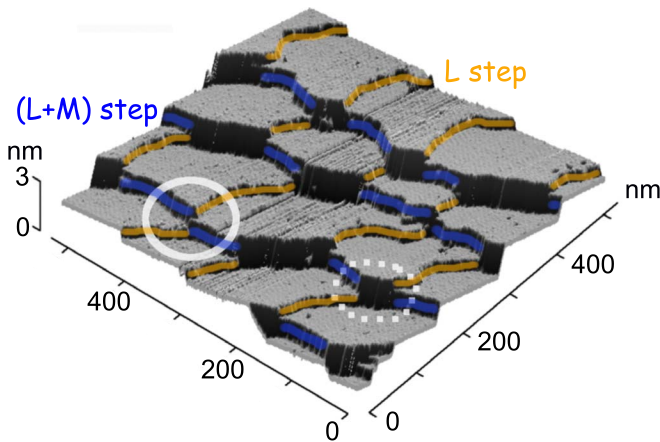


FIG. 3. (Color online) RT STM image of mesh step structure.  $L$  steps (orange overlay) and  $(L+M)$  steps (blue overlay) cross in two different ways, either without overlapping (solid circle) or with overlapping (dotted circle) segment of height  $(2L+M)$ . The former gives a local rhomboidal mesh and the latter gives a local hexagonal mesh.

above and below the step are different, uniformly spaced steps trains or step bunches can be the steady-state surface morphology depending on the sign of the barrier-height difference and the direction of flux to the surface. The ratio of step velocities in this scenario would depend on the relative sizes of the Schwoebel barriers (as well as the step height and local step orientation).

Interpreting the rhomboidal mesh in more detail requires determining the two step heights. LEEM does not directly measure step heights. However, LEEM observations during cooling to RT show that the HT rhomboidal mesh is preserved in some regions while other regions develop elongated terraces, such as Fig. 1(b). The RT STM image in Fig. 3 shows a region of preserved rhomboidal mesh. The image confirms that this mesh is indeed composed of steps of two heights, known as  $L$  and  $(L+M)$  steps in the literature.  $L$  and  $M$  steps were measured to be 0.70 and 0.43 nm high, respectively. In addition, the STM image shows different ways  $L$  steps cross  $(L+M)$  steps. When the two step types do not overlap for any significant distance where they cross (solid circle in Fig. 3), a local rhomboidal terrace morphology results. The two step types can also overlap for a distance where they cross, giving a segment of  $(2L+M)$  step (dotted circle) and a local hexagonal terrace morphology. This observation is consistent with the LEEM observation of two types of mesh seen in Fig. 1(a) and confirms the idea that the hexagonal mesh is the first stage of step bunching.

Identifying the step heights allows estimating the amount of material exchanged with the bulk during a temperature change. For  $\Delta T=2.8$  K at 906 K,  $7(L+M)$  steps (step spacing of  $\sim 400$ – $600$  nm) moved past a given point in Fig. 2 while 4–5  $L$  steps (step spacing of  $\sim 300$  nm) moved past the same point, giving a total height change of  $\sim 10$  nm. Assuming the surfaces are the only sink and source of vacancies, this corresponds to a fractional change in density of  $10^{-5}$  for the  $\sim 2$ -mm-thick crystal. This value is unexpectedly high. For example, if the effective vacancy formation enthalpy  $H_f$  was 2.3 eV, as estimated in Ref. 27, the expected

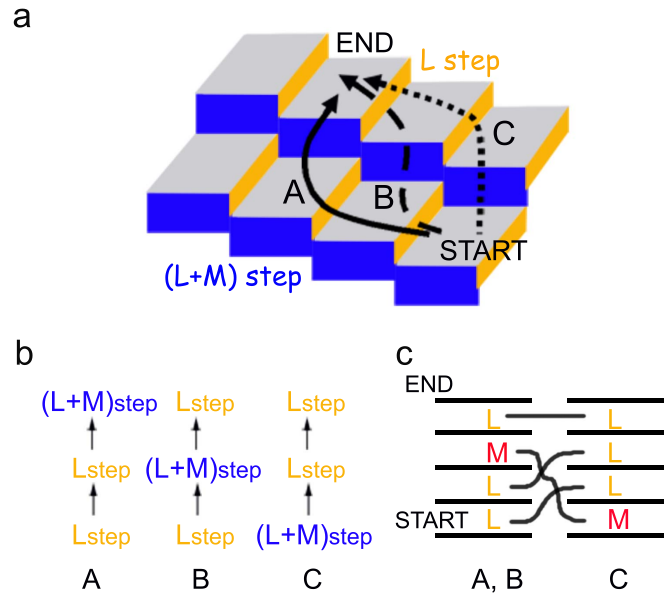


FIG. 4. (Color online) Topology of connecting a periodic, rhomboidal step mesh to bulk layers underneath. (a) Three possible paths from the START to the END terrace. (b) The steps crossed on the paths are A:  $L_{\text{step}}-L_{\text{step}}-(L+M)_{\text{step}}$ , path B:  $L_{\text{step}}-(L+M)_{\text{step}}-L_{\text{step}}$ , and path C:  $(L+M)_{\text{step}}-L_{\text{step}}-L_{\text{step}}$ . (c) Bulk-layer sequence consistent with paths A and B (left) and C (right). Lines between the two stacking sequences show how switching the order of  $L$  and  $M$  layers along path C allows a periodic step array to be connected to underlying bulk layers.

change would be only  $\sim 10^{-14}$ , assuming the vacancy density is proportional to  $\exp(-H_f/kT)$ . The observed height change gives  $H_f=0.6$  eV, which is an upper bound since internal sinks/sources would reduce it.

A striking attribute of a surface covered by a mesh of crossing steps is that the step sequence crossed in traversing the surface depends explicitly on the path chosen. For example, in Fig. 4, a path can be selected that only crosses  $L$  steps. Another selected path only crosses  $(L+M)$  steps. In fact, an arbitrary sequence of  $L$  and  $(L+M)$  steps can be followed including paths that follow a Fibonacci sequence of step heights as well as paths that do not.

Next we propose that stacking defects are needed to connect the observed periodic arrays of surface steps to the underlying bulk layers. Figure 4 shows the topological problem that arises when attempting to find a bulk-layer sequence that is consistent with the mesh of surface steps. Choosing two terraces (START and END) arbitrarily on the rhomboidal mesh, consider three example paths: A (solid), B (dashed), and C (dotted). Figure 4(b) gives the step sequence crossed going from START to END: path A,  $L_{\text{step}}-L_{\text{step}}-(L+M)_{\text{step}}$ ; path B,  $L_{\text{step}}-(L+M)_{\text{step}}-L_{\text{step}}$ ; and path C,  $(L+M)_{\text{step}}-L_{\text{step}}-L_{\text{step}}$ . For paths A and B to cross over the same underlying layers from the START to the END terraces, the layer sequence crossed must be LLML [Fig. 4(c) left]. However, the bulk-layer sequence along path C requires the  $M$  layer to be one of the first two layers, i.e., the sequence must start with either LM or ML layer because the first step along path C is a  $(L+M)$  step. Thus, there is no single way of stacking  $L$  and  $M$  layers that is consistent with the step se-



quences along all three paths. The observed surface with its periodic step arrays, therefore, cannot simply result from truncating a definitive (single) bulk-layer sequence.

An attempt to resolve this topological dilemma is shown in Fig. 4(c). Suppose the sequence of layers crossed at step edges along path C is MLLL. [LMLL is also consistent with Fig. 4(a).] If L and M layers are exchanged underneath the terraces along path C, as sketched in Fig. 4(c), the same stacking sequence inferred above from paths A and B can be obtained. This type of stacking defect corresponds to the phason wall defects found in bulk *i*-Al-Pd-Mn.<sup>11,28</sup> In a tiling description, phasons are visualized as configurational flips leading to local matching-rule violations<sup>29,30</sup> and a planar agglomeration of phasons is a “phason wall.” Because phasons are low-energy defects in the QC bulk, perhaps they occur to allow low-energy (or high-entropy) surface terminations. However, the spatial configuration of phasons (walls) required to create the observed uniform step arrays cannot be uniquely deduced from our experiments. Other types of stacking defects (such as inserted S=L–M layers) might be involved.<sup>31</sup>

To summarize the *i*-Al-Pd-Mn surface at HT: steps of two heights, L and (L+M), move with different velocities when mass flows from the surface to the bulk during cooling. The

two step types move in different directions, apparently independently of each other. The steady-state surface morphology is periodic arrays of the two steps in the form of a rhomboidal mesh. These periodic step arrays are not compatible with the Fibonacci sequence of steps with two heights expected from a bulk-truncated QC.<sup>17</sup> Further evidence against bulk truncation at HT is the uniformity of LEEM intensity, which suggests that each terrace is similarly terminated, unlike the bulk structure. The uniform termination and nonbulklike stacking of the surface may have important consequences for QC growth. For example, step motion and perhaps nucleation<sup>32–34</sup> on a periodic surface is not subject to the severe constraints on step configurations imposed by bulk-truncated models.

This work was supported by the Office of Science, Basic Energy Sciences, Materials Science and Engineering Division of the U.S. Department of Energy (USDOE) under Contracts No. DE-AC02-07CH11358 (Ames), No. DE-AC02-05CH1123 (LBNL), and No. DE-AC04-94AL8500 (Sandia). We thank W. Theis for sharing LEEM data from ELETTRA (Trieste, Italy) and D. Gratias for fruitful discussions about phason walls.

- <sup>1</sup>K. F. McCarty, J. A. Nobel, and N. C. Bartelt, *Nature (London)* **412**, 622 (2001).
- <sup>2</sup>P. A. Thiel, *Prog. Surf. Sci.* **75**, 191 (2004).
- <sup>3</sup>T. M. Schaub, D. E. Bürgler, H.-J. Güntherodt, and J. B. Suck, *Phys. Rev. Lett.* **73**, 1255 (1994).
- <sup>4</sup>M. Gierer, M. A. Van Hove, A. I. Goldman, Z. Shen, S.-L. Chang, C. J. Jenks, C.-M. Zhang, and P. A. Thiel, *Phys. Rev. Lett.* **78**, 467 (1997).
- <sup>5</sup>M. Gierer, M. A. Van Hove, A. I. Goldman, Z. Shen, S.-L. Chang, P. J. Pinhero, C. J. Jenks, J. W. Andereg, C.-M. Zhang, and P. A. Thiel, *Phys. Rev. B* **57**, 7628 (1998).
- <sup>6</sup>Z. Papadopolos *et al.*, *Phys. Rev. B* **66**, 184207 (2002).
- <sup>7</sup>L. Barbier, D. Le Floc’h, Y. Calvayrac, and D. Gratias, *Phys. Rev. Lett.* **88**, 085506 (2002).
- <sup>8</sup>R. D. Diehl *et al.*, *J. Phys.: Condens. Matter* **15**, R63 (2003).
- <sup>9</sup>J. Ledieu *et al.*, *Surf. Sci.* **583**, 4 (2005).
- <sup>10</sup>R. Mikulla, J. Stadler, F. Krul, H.-R. Trebin, and P. Gumbsch, *Phys. Rev. Lett.* **81**, 3163 (1998).
- <sup>11</sup>F. Momprou, J. Crestou, and D. Caillard, *Mater. Sci. Eng., A* **387-389**, 89 (2004).
- <sup>12</sup>B. Unal, T. A. Lograsso, A. Ross, C. J. Jenks, and P. A. Thiel, *Phys. Rev. B* **71**, 165411 (2005).
- <sup>13</sup>Since Ag islands attach to the lower side of *i*-Al-Pd-Mn steps, we located step edges and established up/downhill directions by observing Ag deposition in LEEM (Ref. 14).
- <sup>14</sup>Y. Sato, B. Unal, *et al.* (unpublished).
- <sup>15</sup>M. Boudard *et al.*, *J. Phys.: Condens. Matter* **4**, 10149 (1992).
- <sup>16</sup>A. Yamamoto, *Phys. Rev. Lett.* **93**, 195505 (2004).
- <sup>17</sup>B. Unal, C. J. Jenks, and P. A. Thiel, *Phys. Rev. B* **77**, 195419 (2008).
- <sup>18</sup>J. B. Hannon, J. Sun, K. Pohl, and G. L. Kellogg, *Phys. Rev. Lett.* **96**, 246103 (2006).
- <sup>19</sup>In the different structural models of *i*-Al-Pd-Mn QC, the bulk can be classified into groups of self-similar planes where the QC surface exposes certain groups of atomic planes as preferred terminations at RT. Within a preferred termination for a given model, the atomic density and composition vary by up to ~20% (Refs. 4, 5, 15, and 17).
- <sup>20</sup>N. Shramchenko and F. Denoyer, *Eur. Phys. J. B* **29**, 51 (2002).
- <sup>21</sup>V. Fournée, A. R. Ross, T. A. Lograsso, J. W. Andereg, C. Dong, M. Kramer, I. R. Fisher, P. C. Canfield, and P. A. Thiel, *Phys. Rev. B* **66**, 165423 (2002).
- <sup>22</sup>Ph. Ebert, M. Yurechko, F. Kluge, T. Cai, B. Grushko, P. A. Thiel, and K. Urban, *Phys. Rev. B* **67**, 024208 (2003).
- <sup>23</sup>The observed step spacings varied from ~200 to 600 nm. Over several microns, the spacings were fairly uniform. The mesh structure was disrupted near defects.
- <sup>24</sup>As will be discussed elsewhere (Ref. 14), decreasing the temperature below where differing terrace contrasts appear (~750 K) causes the steps to rearrange into rectangular arrays.
- <sup>25</sup>See supplementary material at <http://link.aps.org/supplemental/10.1103/PhysRevB.81.161406> for data set that gives step velocity ratios of ~1.1 to ~1.5.
- <sup>26</sup>R. L. Schwoebel and E. J. Shipsey, *J. Appl. Phys.* **37**, 3682 (1966).
- <sup>27</sup>K. Sato, F. Baier, A. A. Rempel, W. Sprengel, and H.-E. Schaefer, *Phys. Rev. B* **68**, 214203 (2003).
- <sup>28</sup>M. Feuerbacher and D. Caillard, *Acta Mater.* **54**, 3233 (2006).
- <sup>29</sup>J. E. S. Socolar, *J. Phys. (Paris)* **47**, C3-217 (1986).
- <sup>30</sup>M. Widom, *Philos. Mag.* **88**, 2339 (2008).
- <sup>31</sup>D. Caillard *et al.*, *Philos. Mag. A* **80**, 237 (2000).
- <sup>32</sup>C. L. Henley and R. Lipowsky, *Phys. Rev. Lett.* **59**, 1679 (1987).
- <sup>33</sup>J. Toner, *Phys. Rev. Lett.* **64**, 930 (1990).
- <sup>34</sup>M. A. Fradkin, *Philos. Mag. Lett.* **69**, 71 (1994).